High-frequency low-blaze-angle Mo/Be diffraction gratings — efficiency study

© L.I. Goray,[1,2,3,4] A.S. Dashkov,[1,2] N.A. Kostromin,[1,2] D.V. Mokhov,[2] T.N. Berezovskaya,[2] K.Yu. Shubina,[2]
E.V. Pirogov,[2] V.A. Sharov,[5] S.A. Garakhin,[6] M.V. Zorina,[6] R.S. Pleshkov,[6] N.I. Chkhalo,[6] A.D. Bouravleuv[1,3,4,5]

[1] St. Petersburg State Electrotechnical University „LETI“
197022 St. Petersburg, Russia
[2] Alferov Federal State Budgetary Institution of Higher Education and Science Saint Petersburg National Research Academic
University of the Russian Academy of Sciences,
194021 St. Petersburg, Russia
[3] Institute for Analytical Instrumentation, Russian Academy of Sciences,
198095 St. Petersburg, Russia
[4] AN HEO „University associated with IA EAEC“
199226 St. Petersburg, Russia
[5] Ioffe Institute,
194021 St. Petersburg, Russia
[6] The Institute for Physics of Microstructures, Russian Academy of Sciences,
603087 Afonino, Kstovsky District, Nizhny Novgorod Oblast, Russia
e-mail: lig@pcgrate.com

The paper presents the results of studies of the diffraction efficiency of blazed gratings, carried out by modelling in the PCGrate[TM] code using groove profile shapes obtained by atomic force microscopy and measurements on the laboratory reflectometer with a high-resolution Czerny-Turner spectrometer. High-frequency diffraction gratings with a density of 2500 mm^{-1} and a small inclination angle of the reflecting facet were fabricated on Si(111)1.8° wafers using electron beam lithography and anisotropic wet etching. A grating with a blaze angle of ~1.7°, coated with 40 Mo/Be bilayers, demonstrated in the classical mount an absolute diffraction efficiency of ~38% in minus second order at an incident angle of 3° of unpolarized radiation at a wavelength of 11.3 nm. Taking into account the measured reflectance of the multilayer coating ~0.6, the maximum relative (grating) efficiency was ~63%.

Introduction

Reflective X-ray diffraction triangular-profile („blazed“) gratings are used in the inelastic resonant X-ray scattering spectroscopy, projection lithography in the extreme ultraviolet range (EUV) and beyond it, in space mission instruments, at X-ray free-electron laser stations (XFEL) and fourth-generation synchrotron radiation (SR) sources. One can achieve high absolute diffraction efficiency η (i.e., obtained considering the coating material reflectance) of high-frequency X-ray blazed gratings, especially those operating in the short-wavelength region of the tender X-ray (TX) range, when two conditions are present: (1) low blaze angle α; (2) multilayer coating — for increase in η and/or critical angle in the classical diffraction mount [1,2]. Groove depth of similar high-frequency multilayer low blaze angle gratings (HFMLBG) shall be within the range of several nanometers to several tens nanometers and their profile shall not vary after application of the multilayer coating.

In [3], anisotropic etching was used to make Mo/Si HFMLBG -5250 mm^{-1} with $\alpha = 2°$ and its measured absolute -diffraction efficiency of $n = 1$ order was $\eta(-1) = 40\%$ at $\lambda = -13.3$ nm. In [4], W/B$_4$C HFMLBG 2500 mm^{-1} with $\alpha = -1.75°$ was fabricated, for which $\eta(-2) = 13.5\%$ efficiency was -obtained at $\lambda = 1.77$ nm. In [5], for the Cr/C grating 2400 -mm^{-1} with $\alpha = 1°$, $\eta(-1) = 60\%$ was obtained at -$\lambda = 0.4$ nm, as well as at $\lambda = 0.3$ nm.

The need for improvement of multilayer Be-mirrors for advancing the new generation EUV lithography has been formulated relatively recently [6]. In just one decade high results have been achieved in the development, manufacturing, and characterization of Mo/Be and other Be-containing multilayer mirrors not only for lithography but also for space, X-ray microscopy, and other purposes [7–9]. Recently, we have fabricated and investigated multilayer Mo/Be blazed gratings [10]. Grating frequency was 2500 mm^{-1} and they had a relatively high blaze angle $\alpha \sim 3.9°$. In this study, theoretical and experimental methods were applied to determine η of multilayer Mo/Be HFMLBG

$2500\,\mathrm{mm}^{-1}$ with $\alpha \sim 1.8°$ intended for operation in EUV and fabricated using the electron beam lithography, wet anisotropic etching of Si wafers and magnetron sputtering of multilayer coating [11].

1. Absolute diffraction efficiency research methods

The fabricated Mo/Be HFMLBG are designed for operation in a classical optical mount with near-normal incidence ($\theta \sim 0-10°$) of radiation with $\lambda = 11.3$ nm. The absolute diffraction efficiency was obtained herein by computer simulation using realistic (measured using atomic-force microscopy (AFM)) of groove profiles and random roughness taken from [12] the refraction indices as well as direct measurements of the absolute diffraction efficiency using the laboratory EUV reflectometer under unpolarized radiation. The fabrication technology of the diffraction gratings investigated in this work, as well as methods for characterizing their morphology (shape of grooves, thickness of layers, interlayer roughness/diffuse interfaces) are presented in a separate article [13].

1.1. Grating design

The grating blaze may be characterized using a simple geometrical model — according to the classical (in-plane) diffraction grating equation [14]:

$$\sin\theta_n - \sin\theta = n\frac{\lambda}{d}, \quad n = 0, \pm1, \pm2, \ldots, \quad (1)$$

where n is the diffraction order, $n \in Z$, θ and θ_n are the incidence and diffraction angles, respectively, counted from the normal (signs of angles are chosen according to the Cartesian agreement).

If the mirror wave reflected from the grating groove facet coincides in direction with the n-the diffraction order propagation direction, then

$$2\alpha = \xi_{\mathrm{dif}} - \xi_{\mathrm{inc}}, \quad (2)$$

where $\xi_{\mathrm{inc}} = 90° - |\theta|$, $\xi_{\mathrm{dif}} = 90° - |\theta_n|$. Condition (2) describing the enhancement of a certain order of diffraction is known as the grating blaze (resonance). It apparently does not depend either on the wavelength or on the grating period and determines the correlation between the blaze angle of the reflective facet and the radiation incidence and diffraction angles. This is a very general geometrical property of the scattering theory that is typical not only for gratings, but also for quasiperiodic scatterers such as self-organizing particles (quantum dots) with clearly defined crystal faces, and random roughnesses with a triangular diffuser profile.

The asymptotic theory of diffraction predicts the achievement of 100% relative (grating) diffraction efficiency (i.e. obtained considering an ideal conductance of the grating material) for diffraction order n at blaze wavelength λ_{blaze} in TM incident polarization for the triangular groove profile with right apex angle on condition that [15]:

$$|n|\lambda_{\mathrm{blaze}} = 2d\sin\alpha. \quad (3)$$

For the Bragg mode with number k, the multilayer coating period Λ is defined from the Bragg-Wulff condition:

$$2\Lambda\cos\theta = k\lambda. \quad (4)$$

Hence, the required Λ for HFMLBG may be easily estimated using (1) for any diffraction order and blaze angle [2]:

$$\Lambda = d\sin\alpha/(|n|k). \quad (5)$$

From (5) in accordance with the scalar diffraction theory predictions, a grating with $d = 400$ nm, $\alpha \approx 1.65°$ and blaze for $n = -2$ shall have multilayer coating with $\Lambda = 5.7$ nm when used in the first Bragg order. For high-frequency, even shallow, gratings, this is a rough estimate [2,16] and shall be updated by direct numerical calculations using electromagnetic diffraction theory and realistic groove profile as described below. Taking into account this remark, the magnitude of the maximum of the absolute diffraction efficiency depends on the compliance accuracy of (5) and antiblaze (HFMLBG absorption) angle effect consideration [17].

1.2. Absolute diffraction efficiency simulation

Diffraction properties of the HFMLBG to be manufactured with the AFM-measured boundary profiles were examined using the well-proven modified boundary integral equation method [18] and PCGrate™ software [19]. Electromagnetic radiation diffraction on the grating problem is reduced to solution of the Helmholtz vector equation with rigorous boundary conditions and radiation conditions. To solve this problem, we use a multi-purpose and high-precision boundary integral equation method that was modified for a short-wave range and generalized for randomly rough surfaces. As a result, the problem of 3D-plane-wave diffraction on a general grating presented as an infinite single-periodic structure is limited to the Helmholtz system of equations for one of the electric and magnetic field components in $\mathbb{R}^2$, solutions for which are quasiperiodic in one direction, satisfy the condition of radiation with respect to other direction and jumps at the interfaces between the layers of the grating. For conical diffraction, as opposed to to the classical one, boundary values of the identified field components, as well as their normal and tangential derivatives, are related. The method uses only boundary data from which both near and far fields are found.

It turned out that the modified integral method (MIM) can easily solve complex reflection and transmission diffraction problems not only in a single-mode operation (one intense diffraction order) and at angles close to or smaller than the total external reflection angle (counted from the

grating surface) for this material, but also with enormous number of orders, arbitrary incident light geometry/polarization and any grating parameters. In other words, such input parameters of the diffraction problem for which not only all known approximate or asymptotic calculation methods for absolute diffraction efficiency of gratings and diffusion scattering intensity, but also most rigorous methods are not applicable. MIM together with the stochastic analysis based on the Monte Carlo method [20] are used not only to simulate η gratings with realistic parameters, but also to determine the scattered light intensity and absorbed energy magnitude. In addition, the developed and widely used boundary integral equation method is applicable, due to fast convergence, to a much more complex diffraction problem — (optimization) synthesis problem that has been already tested on various types of gratings, including those intended for space equipment and terminal XFEL stations [17,21]. The study will develop a similar approach to design and analysis of η HFMLBG. Modern computers (work stations with multithread CPU and high-performance graphics cards) and algorithms with code optimization and parallelizing are used to increase the corresponding simulation rate by several orders of magnitude which also indicates that this approach is promising for solving heavy inverse scattering problems [22]. Due to the flexibility and accuracy of PCGrate^{TM}, almost any scattering problems on periodic, quasiperiodic and random nanoreliefs can be solved, though sometimes this requires considerable computational resources [17]. Thus, the abovementioned theoretical analysis and synthesis methods used herein make it possible not only to significantly reduce the cost of the expensive experiments of manufacturing of high quality HFMLBG with the predefined grooves (boundaries) profile, but also to replace to a great extent and/or supplement labour-intensive measurements of the absolute diffraction efficiency that are usually conducted at SR sources.

To examine the boundaries of the produced HFMLBG with random roughness, statistical averaging of the radiation scattering intensity by the Monte Carlo method was used. When solving the grating scattering problem, realistic parameters of the grating layers were used as input data (boundary profile shape, roughness, density of material, interface diffusivity). As a result, the calculations of the absolute diffraction efficiency of the grating orders not only the averaged shape (polygonal — derived from microscopic measurements or by growth process simulation) of its layer boundaries was considered, but also the random interface roughness resulting in reduction of η due to the diffusion scattering intensity. The approximations were used only at the numerical solution stage (infinite series/matrix truncation and process convergence estimation). It should be noted that, to define the radiation scattering intensity on random and random-periodic reliefs, procedure convergence and accuracy shall be controlled not only by the number of discretization (collocation) points, but also by the number of

random samples (sets of random boundaries) in the Monte Carlo method.

1.3. AFM measurement of realistic groove profiles

To ensure repeatability and comparability of the simulation results obtained for the absolute diffraction efficiency of various gratings, we have developed and tested realistic profile (averaged profile of a single groove and random profiles with lengths of several periods) and roughness (high-frequency and medium-frequency) measurement techniques used to calculate η of the gratings in PCGrate^{TM}. For simulation of η without considering random roughness, we use an averaged profile of a single grating groove (Figure 1, a) that is exported with high resolution (> 500 dots) into PCGrate^{TM}.

For simulation of η with rigorous consideration of high-frequency and medium-frequency roughness components with any irregularity statistics (by the Monte Carlo method), we use random (non-averaged) groove profiles with a length of three periods (Figure 1, b) measured in various regions of the grating aperture. Note that such scans include both high-frequency and medium-frequency components of the random roughness, i.e. a random shape of groove profile for short-period gratings. In averaged profiles of a single groove, these components are averaged and the profile is „smoothed" and „aligned", i.e. the profile shape becomes closer to the ideal shape. These techniques are described in more detail in [23]. Such measurements shall be performed both before and after deposition of the multilayer coating.

The abovementioned technique was used to describe the examined HFMLBG by measuring the profiles and roughness in several areas using NT-MDT NTegra Aura atomic-force microscope. All scans had 512×512 points and a semi-contact scanning method was used. Figure 1 shows the AFM profiles of Sv-4-3 grating used in simulation of the absolute diffraction efficiency and scattered radiation intensity.

1.4. Absolute diffraction efficiency measurement

Parameters of the fabricated gratings are listed in Table 1. Based on the obtained parameters and calculation data for η (Table 2), diffraction efficiency measurements of the best (Sv-4-3) grating were performed using the Czerny-Turner high-resolution spectrometer, which has a plane diffraction grating, two spherical collimating mirrors used as a monochromator, and a laser-plasma light source [24]. Absolute diffraction efficiency was measured in various diffraction orders according to the technique used for testing the identical medium-frequency ($d \approx 2\,\mu$m) multilayer Mo/Si-blazed grating for which we obtained a record-breaking $\eta \sim 40\%$ in the -8th order at $\lambda = 13.5\,$nm of non-polarized radiation [25]. With measurements at $\lambda = 11.3\,$nm, the radiation incidence angle was close to the normal to the grating plane and was equal to $3° - 8°$.
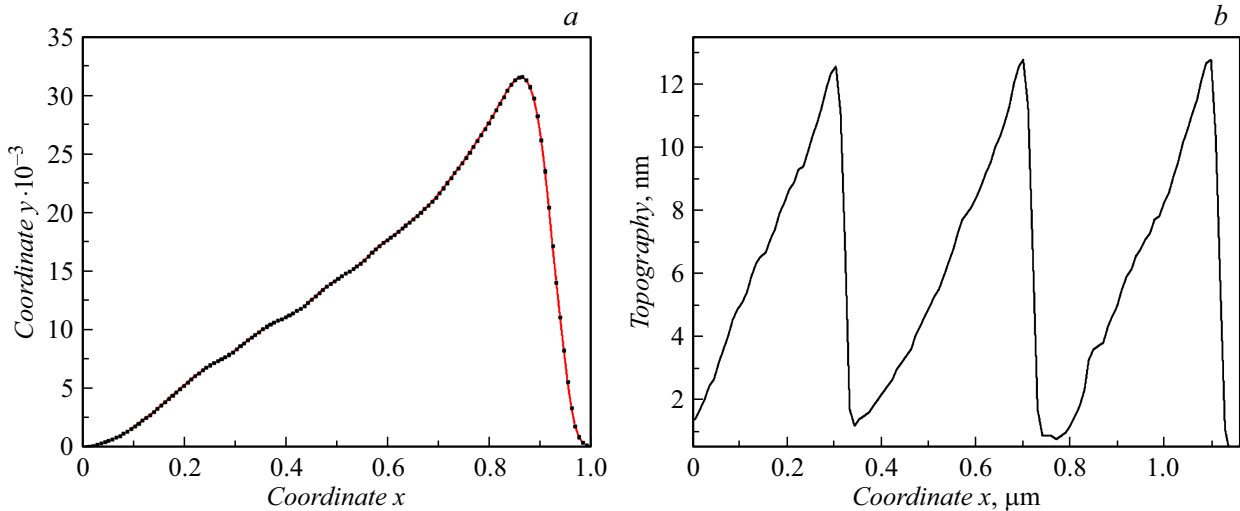
Figure 1. AFM- measured profiles of Sv-4-3 grating grooves: *a* — averaged profile of a single groove; *b* — random profile with a length of three periods.

Table 1. Parameters of the fabricated gratings

Grating	Groove depth, nm	Reflecting facet length, nm	Blaze angle, °	Mo/Be coating thickness nm	Roughness, Rms, nm	
					$(1 \times 1 \, \mu m^2)$	$(20 \, \mu m)$
Sv-4-1	11.0	345	1.8	230	0.45	0.69
Sv-4-3	11.0	356	1.8	230	0.39	0.70

Table 2. Absolute diffraction efficiency (η) of gratings

Grating	$\eta(-2)$, %			
	Calculation for the ideal grating	Calculation without roughness	Calculation with roughness	Measurement
Sv-4-1	66.0	53.7	−	−
Sv-4-3		59.7	29.0	38.0

2. Findings and discussion

Theoretical (simulations) and experimental (measurements) methods were used to determine η of Sv-4-1 and Sv-4-3 gratings for $\lambda = 11.3$ nm nonpolarized radiation in the classical mounting (in the dispersion plane). For comparison, Figure 2 shows first-order diffraction efficiency curves of the ideal 40-bilayer Mo/Be grating with a multilayer coating period of $\Lambda = 5.7$ nm at the incidence angle θ range from $0.5°$ to $9.5°$ simulated using the ideal triangle boundary profile with $\alpha = 1.8°$ and antiblaze angle $\beta = 25°$. As follows from the above graphs, $\eta(-2) \approx 66\%$, and the efficiency of the nearby orders is several orders of magnitude lower.

Figure 3 shows curves of the absolute diffraction efficiency of the orders from 0 to -3 of Sv-4-3 grating for $\lambda = 11.3$ nm and θ within $0.5° - 9°$ simulated using the averaged profile of a single groove (without taking into account reflective facet roughness). The curves in Figure 3 show that $\eta(-2) \approx 60\%$, i.e. only 10% less than that of the ideal grating. And the efficiency of the nearby orders is several orders of magnitude lower, including the zero order. The maximum theoretical η of Sv-4-1 grating determined using the averaged groove profile turned out to be 6% lower (Table 2).

The absolute diffraction efficiency in the -2nd order calculated using the AFM-measured in several areas of Sv-4-3 grating (with random roughness) random profiles was $\sim 29\%$ at $\lambda = 11.3$ nm (Figure 4), i.e. half as much as η calculated for the averaged groove profile without random roughness — both high-frequency and medium-frequency, i.e. considering the random groove profile shape. Note
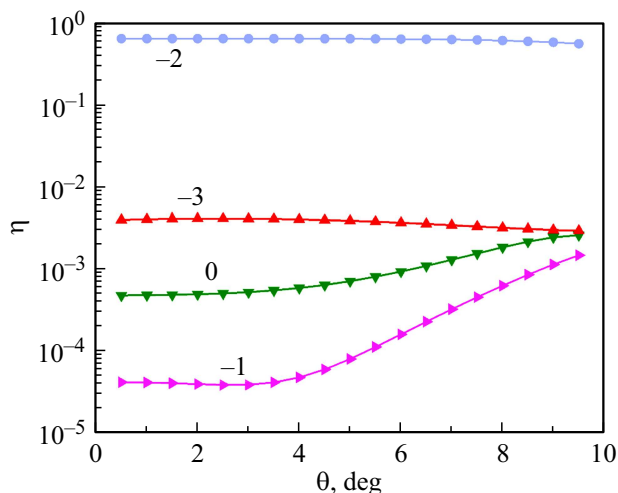
Figure 2. Absolute diffraction efficiency of the orders of the ideal 40-bilayer Mo/Be multilayer grating with $\Lambda = 5.7$ nm and triangle boundaries with $\alpha = 1.8°$ and $\beta = 25°$ for $\lambda = 11.3$ nm vs the angle of incidence.
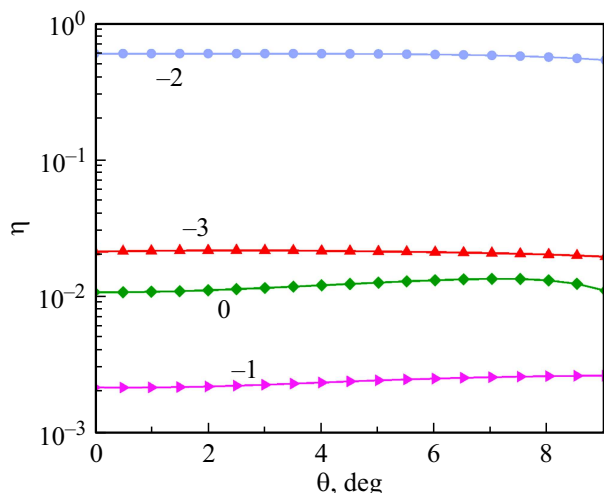
Figure 3. Absolute diffraction efficiency of the orders of Sv-4-3 (Mo/Be) grating at $\lambda = 11.3$ nm in dependence on the incidence angle (without roughness).

that the such value of η may considerably depend on the randomly chosen grating areas (in the center, at the edges).

When measuring Sv-4-3 grating, the maximum absolute diffraction efficiency $\sim 38\%$ in the -2nd order was detected at the wavelength of 11.3 nm in the classical optical mount with incidence angle $\theta = 3°$ and detector angle $177°$ (Figure 5), that corresponds to the theoretical diffraction angle $\theta(-2) = -0.2°$ within $0.1°-0.2°$ accuracy. The diffraction efficiency measured in the -2nd order at large incidence angles decreases gradually with the incidence angle and is equal to $\sim 30\%$ at $\theta = 8°$ (Figure 5) that agrees well with the theoretical values.

To investigate the homogeneity of the measured diffraction efficiency, the reflectivity was estimated by moving Sv-

4-3 grating using coordinate movement perpendicular to the grooves (as far as the used movement permits), and at the fixed incidence angle $\theta = 5°$. Figure 6 shows the curve of $\eta(-2)$ measured at a non-polarized radiation wavelength of $\lambda = 11.3$ nm in the classical mount in dependence on the table coordinate during scanning of Sv-4-3 grating. Figure 6 shows that during grating scanning at 11 mm length (table coordinate varies from 189 to 200 mm), $\eta(-2)$ varies from 0.28 to 0.36. Thus, the heterogeneity of absolute diffraction efficiencies calculated as the ratio of the RMS deviation to the average value is equal to $\pm 8.3\%$.

Table 2 shows maximum values of η of the investigated gratings obtained by: 1) simulation in PCGrate^{TM} for the
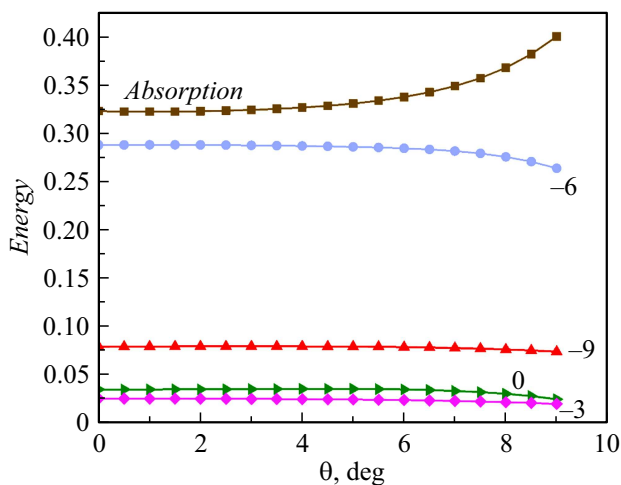
Figure 4. Absolute diffraction efficiency of the orders (the numbers are multiplied by 3) and absorption of Sv-4-3 (Mo/Be) grating at $\lambda = 11.3$ nm in dependence on the incidence angle (with roughness).
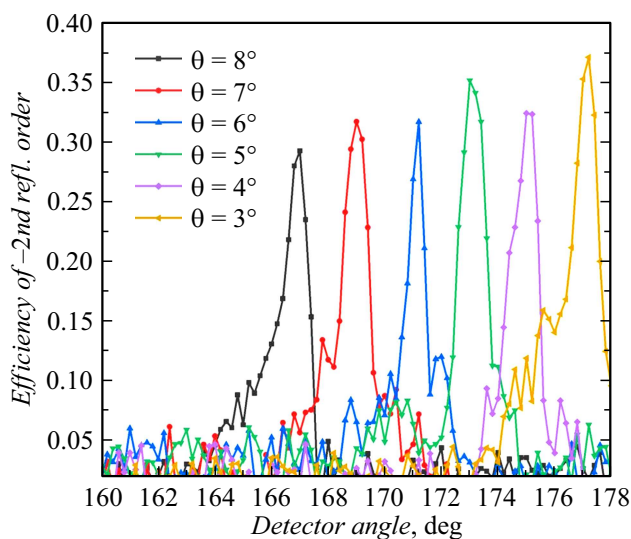
Figure 5. Absolute efficiency of the -2nd order of Sv-4-3 grating measured under the non-polarized radiation with $\lambda = 11.3$ nm in the classical mount at $\theta = 3°-8°$ in dependence on the detector scanning angle.
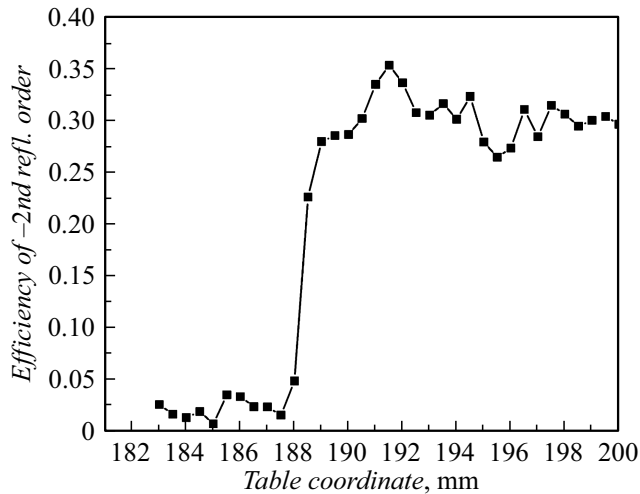
Figure 6. Dependence of the absolute efficiency of the -2nd order of Sv-4-3 grating measured in the non-polarized radiation with $\lambda = 11.3$ nm in the classical mount at $\theta = 5°$ on the table coordinate during grating movement.

ideal grating with identical parameters; 2) simulation in PCGrate^{TM} for the manufactured grating without random roughness of the reflecting facet surface; 3) simulation in PCGrate^{TM} for the fabricated grating with random roughness of the reflecting facet surface; 4) measurements of the prepared grating using the reflectometer at a wavelength of 11.3 nm. Table 2 shows that for Sv-4-1 grating the calculated value of η is 6.0% lower than for Sv-4-3 grating, that may be explained by a shorter reflecting facet. The maximum reflectance for the chosen multilayer coating with $N = 40$ is $R = 0.72$; therefore, the relative diffraction efficiency of the ideal grating is 91.7%, and the maximum relative diffraction efficiency of Sv-4-3 grating according to the simulation with a realistic profile, but without random roughness, is 82.9%, which is 8.8% lower than the theoretically achievable calculated value. This means that the mean profile of Sv-4-3 grating is close to the ideal triangular asymmetric profile.

The maximum reflectance of the applied Mo/Be coating by the test measurements was ∼0.60; thus, the maximum relative efficiency of Sv-4-3 grating according to the measurements was 63.3%, which is 19.6% lower than the theoretical value taking into account the AFM-measured averaged groove profile. Such deviation of the measured efficiency from the simulated value for the realistic profile is caused by: 1) matching error between the grating groove profile and multilayer coating period; 2) radiation scattering on the surface irregularities (random roughness); (3) absence of the pattern (reflecting facets) at $5-7\%$ of the grating area due to stitching during electron lithography mask recording [13]; 4) curvature of the reflecting facet due to not fully removed Si nubs (not all reflecting facet length is used) [26]; 5) groove inhomogeneity across the grating aperture.

Conclusion

Theoretical and experimental studies of the diffraction efficiency of high-frequency multilayer Mo/Be gratings with $d \sim 400$ nm and low blaze angle $\sim 1.7°$ were conducted. Simulations were performed using PCGrate^{TM} software, which was developed using a rigorous boundary integral equation method, and averaged and randomly rough groove profiles obtained from the AFM data. The calculations were verified by direct measurements in the EUV range carried out on laboratory equipment using the reflectometer with the Czerny-Turner high-resolution spectrometer. The diffraction blazed gratings were manufactured on Si(111)1.8° wafers using the electron-beam lithography methods and wet anisotropic etching. After deposition of 40 periods of Mo/Be coating with the total thickness of ~ 230 nm by the magnetron sputtering method, the gratings had a triangular asymmetric groove profile close to the ideal one with acceptable roughness of the reflecting facet surfaces, which is supported by the results of the efficiency simulation and profile measurements on the atomic-force microscope.

The measured absolute diffraction efficiency of Sv-4-3 grating was $\sim 38\%$ in the -2nd order at the wavelength of 11.3 nm in the classical optical diffraction mount at incident angle 3° counted from the normal to the grating surface. The maximum relative grating efficiency was $\sim 63\%$, which is by 30% lower than the theoretical efficiency obtained for the ideal triangular groove profile. The analysis shows that the reduction of the efficiency is primarily associated with the presence of random roughness and with mask defectivity (stitching) during production of the Si grating.

Our further efforts will be focused on optimization of electron-beam mask recording modes to remove stitching and to improve the groove profile (reduce random roughness) and grating parameters homogeneity across area. This will increase considerably the relative diffraction efficiency of high-frequency multilayer gratings with low blaze angle and will be significantly increased and will bring it closer to its theoretical limit. If we add to this the improvement of the multilayer coating deposition process to increase the reflectivity, together this will make it possible to achieve record values of absolute diffraction efficiency of HFMLBG — that are essential for various EUV and TX and also hard X-ray range applications.

Conflict of interest

The authors declare that they have no conflict of interest.

References

[1] L. Goray, W. Jark, D. Eichert. J. Synchrotron Rad, **25** (6), 1683 (2018). DOI: 10.1107/S1600577518012419

[2] D.L. Voronov, L.I. Goray, T. Warwick, V.V. Yashchuk, H.A. Padmore. Opt. Express, **23** (4), 4771 (2015). DOI: 10.1364/OE.23.004771

[3] D.L. Voronov, E.M. Gullikson, F. Salmassi, T. Warwick, H.A. Padmore. Opt. Lett., **39** (11), 3157 (2014). DOI: 10.1364/OL.39.003157

[4] D.L. Voronov, F. Salmassi, J. Meyer-Ilse, E.M. Gullikson, T. Warwick, H.A. Padmore. Opt. Express, **24** (11), 11334 (2016). DOI: 10.1364/OE.24.011334

[5] A. Sokolov, Q. Huang, F. Senf, J. Feng, S. Lemke, S. Alimov, J. Knedel, T. Zeschke, O. Kutz, T. Seliger, G. Gwalt, F. Schäfers, F. Siewert, I. Kozhevnikov, R. Qi, Z. Zhang, W. Li, Z. Wang. Opt. Express, **27** (12), 16833 (2019). DOI: 10.1364/OE.27.016833

[6] N.I. Chkhalo, N.N. Salashchenko. AIP Advances, **3** (8), 082130 (2013). DOI: 10.1063/1.4820354

[7] M.V. Svechnikov, N.I. Chkhalo, S.A. Gusev, A.N. Nechay, D.E. Pariev, A.E. Pestov, V.N. Polkovnikov, D.A. Tatarskiy, N.N. Salashchenko, F. Schäfers, M.G. Sertsu, A. Sokolov, Y.A. Vainer, M.V. Zorina. Opt. Express, **26** (26), 33718 (2018). DOI: 10.1364/OE.26.033718

[8] N.I. Chkhalo, S.A. Garakhin, A.Ya. Lopatin, A.N. Nechay, A.E. Pestov, V.N. Polkovnikov, N.N. Salashchenko, N.N. Tsybin, S.Yu. Zuev. AIP Advances, **8** (10), 105003 (2018). DOI: 10.1063/1.5048288

[9] V.N. Polkovnikov, N.I. Chkhalo, R.S. Pleshkov, N.N. Salashchenko, F. Schäfers, M.G. Sertsu, A. Sokolov, M.V. Svechnikov, S.Yu. Zuev. Opt. Lett., **44** (2), 263 (2019). DOI: 10.1364/OL.44.000263

[10] L.I. Goray, T.N. Berezovskaya, D.V. Mokhov, K.Yu. Shubina, E.V. Pirogov, V.A. Sharov, A.S. Dashkov, N.A. Kostromin, M.V. Zorina, M.M. Barysheva, S.A. Garakhin, S.Yu. zuev, K.V. Nikolaev, S.N. Yakunin, B.S.Roshchin, N.I. Chkhalo, V.E. Asadchikov, A.D. Buravlev. Sbornik tez.konf. *„Elektronno-luchevye tekhnologii i rentgenovskaya optika v mikroelektronika" KELT-23* (Chernigolovka, Rossiya, 2023), s. 219.

[11] D.V. Mokhov, T.N. Berezovskaya, K.Yu. Shubina, E.V. Pirogov, A.V. Nashchekin, V.A. Sharov, L.I. Goray. Tech. Phys., **92** (8), 1009 (2022). DOI: 10.21883/TP.2022.08.54564.74-22

[12] Electronic source. Available at: https://henke.lbl.gov/optical_constants/

[13] D.V. Mokhov, T.N. Berezovskaya, E.V. Pirogov, K.Yu. Shubina, N.D. Prasolov, M.V. Zorina, S.A. Garakhin, R.S. Pleshkov, N.I. Chkhalo, A.S. Dashkov, N.A. Kostromin, L.I. Goray, A.D. Buravlev. ZhTF, **94** (7), 2024 (in Russian)

[14] F.M. Gerasimov, E.A. Yakovlev. *Current Trends in Spectroscopy Technology*, ed. by S.G. Rautian (Nauka, Novosibirsk, 1982, in Russian)

[15] E.G. Loewen, E. Popov. *Diffraction Gratings and Applications* (CRC Press, 2018), 630 p.

[16] L.I. Gorai. Bull. Russian Academy Sciences. Physics, **69** (2), 231 (2005).

[17] L. Goray. J. Synchrotron Rad., **28** (1), 196 (2021). DOI: 10.1107/S160057752001440X

[18] L.I. Goray, G. Schmidt. *Gratings: Theory and Numerical Applications* (Presses Universitaires de Provence, Marcel, 2014), Ch. 12.

[19] L.I. Goray, S.Yu. Sadov. Komp'yuternaya programma PCGrate^TM. URL: www.pcgrate.com

[20] D.P. Kroese, T. Taimre, Z.I. Botev. *Handbook of Monte Carlo Methods* (Wiley, 2011), 772 p.

[21] H. Marlowe, R.L. McEntaffer, C.T. Deroo, D.M. Miles, J.H. Tutt, L.I. Goray, F. Scholze, A.F. Herrero, C. Laubis, V. Soltwisch. Appl. Opt., **55** (21), 5548 (2016).

[22] L.I. Goray, A.S. Dashkov, N.A. Kostromin, D.A. Barykin, 2023 Days on Diffraction (DD), Proc. IEEE, 101 (2023). DOI: 10.1109/DD58728.2023.10325796.

[23] L.I. Goray, V.A. Sharov, D.V. Mokhov, T.N. Berezovskaya, K.Yu. Shubina, E.V. Pirogov, A.S. Dashkov, A.D. Bouravleuv. Tech. Phys., **68** (7), 797 (2023). DOI: 10.61011/TP.2023.07.56619.66-23

[24] S.A. Garakhin, N.I. Chkhalo, I.A. Kas'kov, A.Ya. Lopatin, I.V. Malyshev, A.N. Nechay, A.E. Pestov, V.N. Polkovnikov, N.N. Salashchenko, M.V. Svechnikov, N.N. Tsybin, I.G. Zabrodin, S.Yu. Zuev. Rev. Sci. Instrum., **91** (6), 063103 (2020). DOI: 10.1063/1.5144489

[25] L.I. Goray, T.N. Berezovskaya, D.V. Mokhov, V.A. Sharov, K.Yu. Shubina, E.V. Pirogov, A.S. Dashkov, A.V. Nashchekin, M.V. Zorina, M.M. Barysheva, S.A. Garakhin, S.Yu. Zuev, N.I. Chkhalo. Bull. Lebedev Phys. Inst., **50** (2), S250 (2023). DOI: 10.3103/S1068335623140063

[26] L.I. Goray, T.N. Berezovskaya, D.V. Mokhov, V.A. Sharov, K.Yu. Shubina, E.V. Pirogov, A.S. Dashkov. J. Surf. Invest., **17** (1), S104 (2023). DOI: 10.1134/S1027451023070145

Translated by E.Ilinskaya